JOURNAL OF MATERIALS SCIENCE: MATERIALS IN MEDICINE 2 (1991) 153–161

Glass-ceramic–metal composites for making graded seals in prosthetic devices

R. ROGIER*, F. PERNOT
Laboratoire de Science des Matériaux Vitreux – CNRS, URA 1119, USTL, Place E. Bataillon, 34095 Montpellier Cédex 05, France

The possibility of using glass-ceramic–metal composites as graded seals between dense cores of prostheses and a porous glass-ceramic coating, which would promote a direct bond with the bone has been investigated, particularly with respect to thermal and elastic properties. Before binding them to a core, bulk composite materials have been prepared in order to study their properties.

These materials have been obtained from powdered mixtures of a calcium alumino-phosphate glass (CAP) with increasing volume fractions (3.5–50%) of various metals or alloys: titanium, 316 L stainless steel, cobalt-chromium 788 alloy. They have been synthesized by hot pressing immediately followed by a heat treatment to obtain ceramicization of the glass matrix.

Elastic and thermal properties have been determined. The values of elastic moduli and average linear thermal expansion coefficients lie within those of glass-ceramic CAP and those of the corresponding metal. Mechanical properties have been also measured. The material can withstand about four times the body weight when materials are bound to a more rigid metal or alloy.

1. Introduction

During the last two decades, ceramics have been used more and more as medical and dental devices [1–4]. Among these materials, glass-ceramics [5], which are extremely fine-grained ceramics obtained by controlled crystallization of suitable glasses, have received particular attention since 1971 [6]. Such materials with an open porosity have previously been prepared from a calcium alumino-phosphate base glass (CAP) [7, 8]. Living organisms show a good tolerance to these materials. Their porosity allows successful bone ingrowth, and thus a mechanical bond with the bone has been obtained [9]. Their Young's modulus ($\simeq$ 15 GPa) is close to that of bone (18–20 GPa [10]). All these properties lead to the conclusion that such materials could be used to make a coating on the dense metal core of a prosthesis.

The conditions which give a good bonding between the core and this special coating can be compared to those required in a glass-to-metal seal. These requirements can be summarized as [11, 12]: a good adherence between both core and coating (this problem will not be considered in this paper); and a final combination with compressive or very low tensile stresses in the coating.

Stresses develop in a seal during cooling from the set point of the glass to room temperature, because of the thermal mismatch between metal and coating. Their magnitude depends both on thermal and elastic properties of both components [11, 13]. They can lead to fracture when the magnitude of tensile stresses in glass exceeds the strength of the glass.

When an external stress is applied to the seal, the elastic mismatch between glass and metal produces stress concentrations at the interface, which can also induce fractures. This could be the case for a coated hip prosthesis when the patient walks or even remains motionless.

Thermal and/or elastic mismatches are of particular importance because the mechanical strength of the porous coating is rather low ($\simeq$ 20 MPa) [7, 8] and the most probable consequences of a direct bond between this coating and metals commonly used in orthopaedics (titanium and alloys, 316 L stainless steel, cobalt–chromium alloys) will be fractures of the coating or delamination near (or at) the interface.

The coated stem of a femoral prosthesis can be compared to a bead seal, i.e. glass sealed over a metal wire in a concentric cylinder geometry. A method of preventing rupture in these systems consists of carrying out graded seals [12] which reduce the consequences of a too high thermal mismatch: transition glasses have progressively slightly different expansion coefficients. In the same way, in the case of elastic mismatch a gradient of elastic properties could have two effects – to allow a better transmission of stresses between the core and its porous coating and thus to

*Present address: Montpellier Chirurgie, "Le Nobel", Z.A. du Millénaire, 34000 Montpellier, France.

0022–2461/91 $03.00 + .12

prevent fracture at the interface due to elastic mismatch; or to minimize bone atrophy due to mismatch between metal stiffness and surrounding bone [14, 15] which could not be totally damped by the coating.

For the prosthesis such a solution could be used, the intermediate coatings being made of superimposed layers of various glass-ceramic–metal composite materials prepared from mixtures of the base glass CAP and particles of the same metal as the stem of the prosthesis.

In the field of biomedical materials, glass–metal fibre composites have already been proposed as bulk materials [14]. For this reason, high mechanical performances have chiefly been sought. In fact these materials show a marked increase of strength over the parent 45 S 5 bioglass [6] and fractographic analysis also suggests a substantial improvement in toughness.

Materials intended for use as superimposed coatings of different properties do not require such strength and toughness. A prosthesis with its coatings can be considered as a constant strain system, where the most rigid element (the metallic core) imposes its strain on the others. As a result, each layer is subjected to stresses proportional to its elastic modulus. Therefore particulate composites with suitable thermal and elastic properties would be more convenient for this purpose. However, before binding them to core it is necessary to show the possibility of preparing such composites; to measure their thermal and elastic properties, so that their values are actually situated within those of the glass-ceramic and those of the corresponding metal; to determine their mechanical properties for comparison with porous and dense glass-ceramics and metals, and to check that they are statisfactory for materials which must be bound to more rigid ones; and to ensure that their biocompatibility is at least as good as that of the components.

This paper deals with the preparation of materials and the study of their thermal, elastic and mechanical properties.

2. Materials and methods

2.1. The base products

The base glass CAP of the nominal composition P_2O_5 69.0, CaO 22.7, Al_2O_3 8.3 in weight ratio, has previously been used to prepare porous glass-ceramics [7, 8]. Its properties are summarized in Table I. Before melting the glass, the raw materials (calcium bis-dihydrogen phosphate $[Ca(H_2PO_4)_2H_2O]$ and hydrated aluminium orthophosphate $[AlPO_4xH_2O$, $x \leq 35\%$ in weight, determined by TGA]) were mixed and dried at 100 °C for 12 h. They were then introduced in a Pt–10% Rh crucible and melted at 1300 °C for 2 h. The glass was obtained by pouring the liquid onto a cold metal plate; it was then ground and sieved to obtain particles with a size lower than 50 μm.

The metals and alloys were commercial products, their properties, as given by the manufacturers, are also shown in Table I.

2.2. Method of synthesis

Suitable fractions of glass CAP and second phase particles were mixed for 1 h and vacuum hot pressed into composite discs. The pressing instrument and schedule were taken from Decottignies *et al.* [16].

A quantity of mixture calculated to obtain a disc of about 5 mm thick was introduced into a graphite mould, and placed between two pressing pistons in a cylindrical die of 38 mm internal diameter. It was compacted at room temperature under a pressure of 45 MPa. It was then introduced into the press, and when a vacuum of 5×10^{-2} torr was obtained, the temperature was raised to 500 °C and kept constant for 1 h to obtain final dehydration. A densification pressure of 30 MPa was then applied, and the temperature increased up to total sintering ('flash pressing').

Densification was controlled using a micrometer to measure the displacement of the hydraulic ram. As soon as the sample was totally sintered, detected by

TABLE I Properties of components for the preparation of glass-ceramic (CAP)–metal composites

Materials properties		Glass CAP	Glass ceramic CAP	Titanium	316 L Stainless steel	788 Cobalt–chromium alloy
Density (g cm^{-3})		2.64	2.648	4.5	7.95	8.3
Melting point (°C)		–	910	1660	> 1350	> 1400
Average linear expansion coefficients (10^6 °C^{-1})	α_{20-500}	9.3	16.7	8.8 (8.9)	17.5 (16.8)	12.0 (14.4)
	α_{20-700}	–	16.4	– (9.0)	– (17.4)	13.0 (15.2)
Young's modulus (GPa)		64	68	110 (107)	193 (196)	230 (228)
Poisson's ratio		0.256	0.180	0.340 (0.335)	0.300 (0.290)	0.270 (0.250)
Shear modulus (GPa)		25.5	29	41	74	90.5
Bulk modulus (GPa)		43.5	35.5	115	161	166.5
Fracture stress (MPa)				536 [1185]*	520	680
Yield stress (MPa)				454 [1050]*	284	470
Average radius of particles (μm)		≤ 50	–	10	12.5	11

Experimental values in parentheses.

* Both values correspond to TA 6 V titanium alloy.

the arrest of the micrometer, pressure was removed and the sample kept at 700 °C for 1 h to obtain total ceramicization of the matrix.

For each composition, two dense discs were prepared in this way.

2.3. Methods of measurement

2.3.1. Thermal properties

Linear thermal expansion was measured with a differential dilatometer (D.I. 10-2, Adamel–Lhomargy) using vitreous silica as a reference material. Measurements were made from room temperature to 750 °C. Square-shaped samples (15 mm $\leq$ length $\leq$ 25 mm) were cut from hot-pressed discs. A linear heating rate of 3 °C min^{-1} was chosen. From the recorded curves, one can deduce the relative expansion Δ_{samp} of the samples at each temperature

$$\Delta_{samp} = \frac{Y}{KL_0} + \Delta_{sil} \quad (1)$$

where Y = the expansion of the sample at the considered temperature (given by the recorded curve); K = the amplification coefficient of the recorder; L_0 = the initial length of the sample; and Δ_{sil} = relative expansion of the silica at the considered temperature.

It is also possible to deduce the average linear thermal expansion coefficient $\alpha_{T_2-T_1}$ between two temperatures T_1 and T_2

$$\alpha_{T_2-T_1} = \frac{Y_{T_2} - Y_{T_1}}{KL_0(T_2 - T_1)} + \frac{\Delta_{sil-T_2} - \Delta_{sil-T_1}}{T_2 - T_1} \quad (2)$$

2.3.2. Elastic properties

Young's modulus, E, and Poisson's ratio, ν, were determined using dynamic methods. Most measurements were performed by a method based on the magnetostrictive effect [17, 18]. However, a method based on the piezoelectric effect [19] was also used for the smallest samples.

2.3.2.1. Resonance method based on the magnetostrictive effect. The magnetostrictive line consisted of a nickel wire, at one end of which a longitudinal reversible mechanical strain was created. The other end of the wire was introduced and firmly stuck in a small hole machined in the specimen resonator. The resonance frequencies were visualized on a scope from a typical echo. The specimen resonators may be chosen either as square-shaped bars or thin discs.

In square-shaped samples, a small hole was machined at one end along the axis; only longitudinal waves were produced, as long as the length/width ratio was higher than 10. Young's modulus was calculated from the equation

$$E = Dv_e^2 = \frac{2lf_n}{n} \quad (3)$$

where D = density; l = length of the sample; n = order of the resonance frequency; f_n = n order resonance frequency; and v_e = velocity of the burst of waves in the sample. Only Young's modulus can be measured using such samples.

Thin discs were used for the determination of both Young's modulus and Poisson's ratio. Two holes were drilled from the periphery along two perpendicular axes. E and ν are obtained from the frequencies of two vibrational modes: radial and distorsional. Satisfactory measurements require a diameter/thickness ratio of about 10. Poisson's ratio is deduced from a parameter k_1 obtained by the equation

$$k_1 = \frac{f_{1,R} - f_{1,3}}{f_{1,3}} \quad (4)$$

where $f_{1,R}$ = first radial mode frequency; and $f_{1,3}$ = second distorsional mode frequency.

Young's modulus was obtained from Equation 3 in which the velocity v_e is calculated by

$$v_e = v(1 - \nu^2)^{1/2} \quad (5)$$

where v = velocity of the waves in the isotropic disc, which is deduced from the expression

$$v = \frac{2\pi r}{k_2} f(m, n) \quad (6)$$

where $f(m, n)$ = resonance frequency corresponding to m, nodal circle, and n, nodal diameter; r = disc radius; and k_2 = frequency constant depending on resonance frequencies $f(m, n)$.

2.3.2.2. Pulse-echo method based on piezoelectric effect. The magnetostrictive effect method needs samples with a certain volume and a definite form (square-shaped bars or flat discs). The method based on the piezoelectric effect can be used for smaller samples, provided that two polished-parallel flat faces can be obtained.

A thickness vibrating lithium niobate transducer (50 MHz) was cemented to one end of the specimen. This transducer was specially cut to generate both longitudinal and shear waves, and is used both for transmitting and receiving.

The Young's modulus E and Poisson's ratio ν of the specimens were deduced from both velocities of longitudinal, v_e, and shear, v_s, waves and from bulk density, D

$$E = \frac{Dv_s^2(3v_e^2 - 4v_s^2)}{v_e^2 - v_s^2} \quad \text{and} \quad \nu = \frac{v_e^2 - 2v_s^2}{2(v_e^2 - v_s^2)} \quad (7)$$

The knowledge of these two elastic constants permits calculation of the shear, G, and bulk, K, moduli

$$G = \frac{E}{2(1 + \nu)} \quad \text{and} \quad K = \frac{E}{3(1 - 2\nu)} \quad (8)$$

2.3.3. Mechanical properties

Hot-pressed discs were cut with a diamond saw into square-shaped specimens, which were then ground to exact dimensions.

Flexural strength σ_R was determined with an Instron testing machine. Most measurements were made on $1.5 \times 3 \times 15$ mm bars using 3-point loading over a 12 mm span; the loading rate was 0.1 mm mn^{-1}; for each material, 7–16 specimens were thus fractured. Some limited 4-point bend tests were also performed at a loading rate of 0.2 mm min^{-1}, on $2 \times 5 \times 32$ mm bars (2 samples for each material); the inner and outer span were, respectively, 8 and 24 mm. The ground surface of all specimens was stressed to failure. All experiments were carried out in air at room temperature. Three-point, σ_{R3} and 4-point, σ_{R4}, fracture bending stresses were calculated to be

$$\sigma_{R,3} = \frac{3PL_1}{2bw^2} \quad \text{or} \quad \sigma_{R,4} = \frac{3P(L_1 - L_2)}{2bw^2} \tag{9}$$

where P = fracture load; L_1 = outer span; L_2 = inner span; b = sample width; and w = sample thickness.

With $2 \times 4 \times 24$ mm bar specimens, the fracture toughness K_{IC} was determined using the 3-point bend test of a single edge-notched bend specimen (SENB) over a 16 mm span. A notch as thin as possible and of about 1.3 mm depth was machined with a 0.05 mm thickness diamond saw, at the midpoint of one 24 mm edge of each specimen. Notch depth, a, and width, ρ, were measured using special optical microscopes. Specimens were tested at a cross-head speed of 0.05 mm min^{-1}. All measurements were carried out in air at room temperature. For each composite, 2–9 specimens were tested. Fracture toughness was calculated from specimen dimensions, notch depth, a, and fracture load, P, using the equation [20]

$$K_{IC} = \frac{3PL}{2bw^2} Ya^{-1/2} \tag{10}$$

w = sample height.

$$Y = 1.93 - 3.07a/w + 14.53\,[a/w]^2 - 25.11\,[a/w]^3 + 25.80\,[a/w]^4 \tag{11}$$

As shown previously [20, 21] such conditions allow us to reach the 'true' initiating K_{IC} factor.

Knowledge of K_{IC} and Young's modulus, E, allow us to calculate initiating fracture energy Γ_i, which is given by [22]

$$\Gamma_i = \frac{K_{IC}^2}{2E}(1 - \nu^2) \tag{12}$$

3. Results and discussions

3.1. Syntheses

3.1.1. Hot-pressing of glass-ceramic CAP

Pure glass CAP powder without any adjuvant was densified. Sintering begins at about 620 °C and takes place up to 670 °C. At this temperature, when samples thickness reaches a constant value, the viscosity of the glass is so low ($< 10^8$ poises) as pressure must immediately be suppressed to prevent extrusion. Ceramicization treatment was then performed and samples were allowed to cool directly to room temperature without any annealing treatment. In spite of precautions taken, a slight extrusion occurred during pressing, so that samples were difficult to remove from the die.

3.1.2. Hot pressing of composites

Seven or eight compositions with increasing metal volume fractions, c_p, were pressed for each of three types of inclusions (titanium, 316 L stainless steel and cobalt chromium 788 alloy). The final pressing temperature increased with increasing c_p reaching about 750 °C for the richest mixtures; in the same time the sintering rate decreased. Ceramicization treatment followed hot pressing.

For volume fractions up to 50%, all the hot-pressed samples were more than 95% theoretical density and appeared macroscopically homogeneous (Fig. 1). However, for the lowest volume fractions (3.5–10%), as for glass-ceramic, extrusion impeded disc removal from the die and the edges of the discs were slightly chipped. For higher volume fractions (20–50%), discs were easier to remove and their edges remained almost clean.

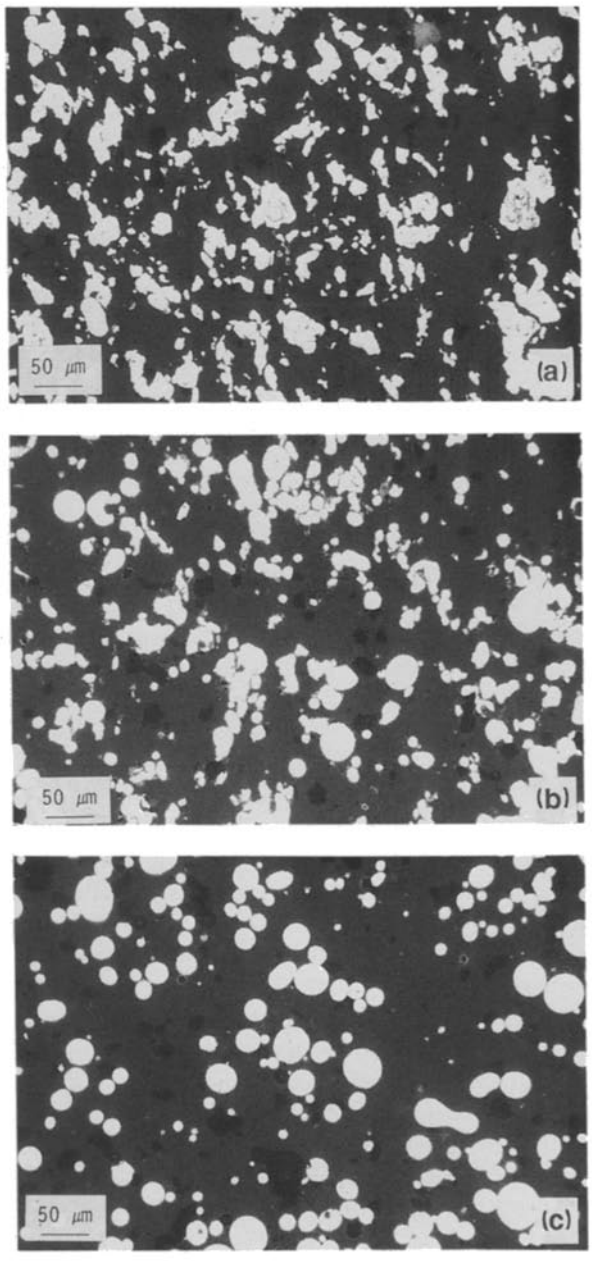

Figure 1 Typical polished surface of various glass-ceramic (CAP)–metal composites. (a) Titanium composites; (b) 316 L stainless steel composites; (c) cobalt–chromium 788 composites.

For volume fractions higher than 50%, poor sintering was obtained and samples tended to crumble.

3.2. Thermal properties

3.2.1. Thermal properties of metallic components

The results are also summarized in Table I (between brackets). In most cases, a good agreement is observed with the data given by the manufacturers; however, a significant difference is noticed for the average linear expansion coefficients of CoCr 788 alloy.

3.2.2. Thermal properties of glass-ceramic CAP and composites

The expansion curves of glass-ceramic CAP and composites (Fig. 2) show a shoulder between 100 and 200 °C which corresponds to structural expansion of phosphates. It is due to $\alpha \rightleftarrows \beta$ transformation of $AlPO_4$ cristobalite form [23–26]. Sometimes other features occur at higher temperatures. Those which were observed close to 500 °C (Fig. $2a_1$) could be due to the residual vitreous phase of the glass-ceramic matrix.

From these curves, various average linear thermal expansion coefficients were calculated. α_{20-700} between 20 and 700 °C was chosen because it can give information about stresses produced in composites during cooling from ceramicization to room temperature. However the values of this coefficient are often disturbed by the features previously reported; that is why α_{20-500} between 20 and 500 °C was also determined. These coefficients are summarized in Table II.

For glass-ceramic–titanium composites, α_{Ti} is much lower than α_{CAP} in both temperature ranges 20–500 °C and 20–700 °C (Table I). As a result, both thermal expansion coefficients of composites decreased as a function of the metal volume fraction c_p. For 316 L composites, these coefficients did not show significant evolution as a function of metal content, since α_{316L} is close to α_{CAP} (Table I).

For CoCr 788 composites, α_{20-500} slightly decreases with metal content. Whatever the values adopted for α_{788}, say: $12 \times 10^{-6}\,°C^{-1}$ (the value given by the manufacturer) or $14.4 \times 10^{-6}\,°C^{-1}$ (the measured values), all the experimental data eventually fall within the coefficient of glass-ceramic and of CoCr 788 alloy. However, some of these experimental coefficients nearly reached α_{788} when it is taken equal to the measured value. It can then be wondered whether the experimental value of α_{788} measured on a dense cylinder is the true coefficient of powdered 788 alloy.

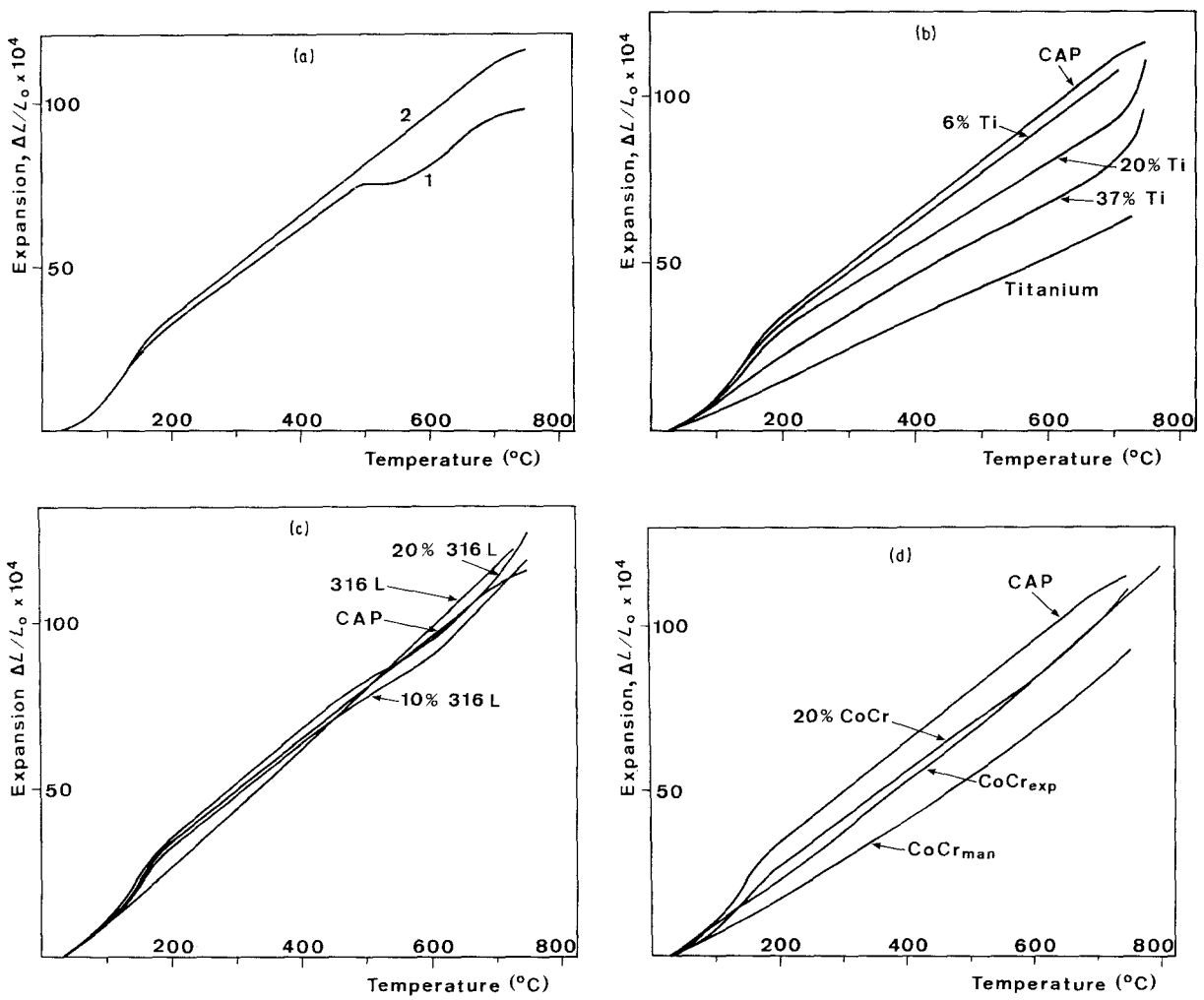

Figure 2 Linear thermal expansion curves of glass-ceramic (CAP)–metal composites. (a) Glass-ceramic with (a_1) or without (a_2) feature close to 500 °C; (b) titanium composites; (c) 316 L stainless steel composites; (d) cobalt–chromium 788 composites.

TABLE II Average linear expansion coefficients of glass-ceramic (CAP)–metal composites

Metal volume fraction %	Ti composites		316 L composites		788 composites	
	α_{20-500}	α_{20-700}	α_{20-500}	α_{20-700}	α_{20-500}	α_{20-700}
0	16.7	16.4	16.7	16.4	16.7	16.4
3.5	16.1	15.5	16.5	19.7	16.0	15.7
6	15.9	15.7	16.2	17.8	15.9	16.2
10	14.4	13.8	16.5	16.1	15.6	15.5
20	14.1	13.4	17.1	16.6	15.2	15.3
30	12.0	11.5	17.2	17.5	14.6	14.8
37	12.2	11.7	16.6	16.9	14.6	14.5
50	11.5	11.4	17.5	18.0	14.5	15.0
Ti	8.9	9.0	–	–	–	–
316 L	–	–	16.8	17.4	–	–
788	–	–	–	–	14.4 (12.0)	15.2 (13.0)

3.3. Elastic properties

3.3.1. Elastic properties of base metals or alloys

The elastic properties of some of the base metals or alloys were controlled; these were measured using the pulse-echo method. The results are summarized (between brackets) in Table I; in all cases, a good agreement was obtained with data of the manufacturers.

3.3.2. Elastic properties of glass-ceramic CAP and composites

Samples of glass-ceramic CAP and composites was cut from hot-pressed discs: square-shaped bars (3 × 5 × 35 mm) and flat discs (diameter, 32 mm; thickness, 3.2 mm). They were used for resonance measurements.

Measurements carried out from both holes drilled at 90° in the discs gave identical resonance frequencies which confirm the homogeneity and isotropy of all materials. A good agreement was obtained between measurements of Young's modulus made on square-shaped bars and discs of the same composition, although these samples were cut from different hot-pressed discs. Good agreement is also noticed between values obtained by resonance and by pulse-echo.

Whatever the system studied, Young's moduli increased with the volume fraction of metal c_p and thus were eventually placed within that of glass-ceramic and that of the corresponding metal. Experimental results are summarized in Table III.

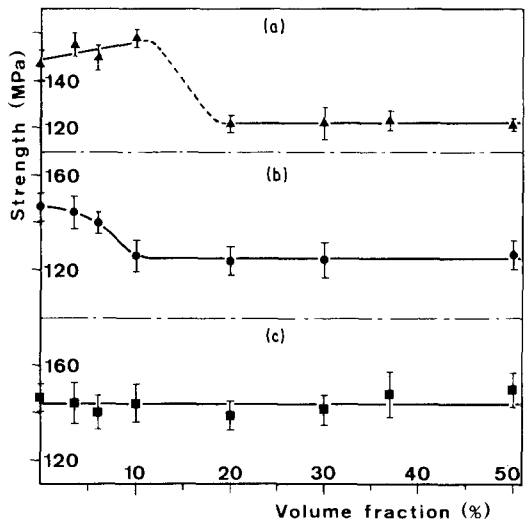

Figure 3 Strength of glass-ceramic (CAP)–metal composites. (a) Titanium composites; (b) 316 L stainless steel composites; (c) cobalt–chromium 788 composites.

TABLE III Elastic properties of glass-ceramic (CAP)–metal composites

Metal volume fraction (%)	Ti composites		316 L composites		788 composites	
	Young's modulus (GPa)	Poisson's ratio	Young's modulus (GPa)	Poisson's ratio	Young's modulus (GPa)	Poisson's ratio
0	68	0.180	68	0.180	68	0.180
3.5	69.5	0.185	72	0.192	70.5	0.191
6	70	0.199	72	0.192	71.5	0.193
10	71	0.195	74	0.196	77.5	0.198
20	71.5	0.203	79	0.204	87.5	0.204
30	73	0.209	88	0.219	98	0.215
37	77	0.220	95	0.222	107	0.223
50	80	0.229	102	0.235	124.5	0.233
Ti	110	0.340	–	–	–	–
316 L	–	–	193	0.300	–	–
788	–	–	–	–	230	0.270

3.4. Mechanical properties

The mechanical properties of three series of composites were studied as a function of the metal volume fraction c_p.

3.4.1. Fracture bending stress

For titanium composites, σ_R slightly increased for low-volume fractions ($c_p \leq 10\%$). For higher metal content ($c_p \geq 20\%$), σ_R remained nearly constant at values lower than the fracture stress, σ_{Rm}, of pure glass-ceramics (Fig. 3a). For 316 L composites, σ_R decreased from 0% to just above 10% inclusions; then it also remained nearly constant between 20 and 50% inclusions (Fig. 3b). For CoCr 788 composites, σ_R did not show significant evolution, remaining close to σ_{Rm} (Fig. 3c).

Comparing the three series of composites, it can be seen that for low volume fractions ($c_p \leq 10\%$)

$$\sigma_{Ti} > \sigma_{CAP} \simeq \sigma_{788} \geq \sigma_{316L}$$

and for higher volume fractions ($c_p \geq 20\%$)

$$\sigma_{CAP} \simeq \sigma_{788} > \sigma_{316L} \simeq \sigma_{Ti}$$

3.4.2. Fracture toughness and fracture energy

For titanium composites, K_{IC} and Γ_i showed similar trends (Fig. 4a and b); they increase from 0–3.5% inclusions; then they decrease up to about 30% inclusions; finally they increase again from 30% inclusions.

For 316 L composites (Fig. 5a and b), K_{IC} and Γ_i also increased from 0 to 3.5% inclusions. A discontinuity was then observed between 3.5 and 6% inclusions on both curves. Finally K_{IC} slightly increases, while Γ_i slightly decreased from 6 to 50%.

For CoCr 788 composites (Fig. 6a and b), K_{IC} remained nearly constant from 0 to 50% inclusions, while Γ_i continuously decreases. A comparison between the three series of composites shows that

$$(K_{IC})_{Ti} > (K_{IC})_{788} \simeq (K_{IC})_{CAP} > (K_{IC})_{316L}$$

$$(\Gamma_i)_{CAP} \simeq (\Gamma_i)_{Ti} > \begin{cases} (\Gamma_i)_{788} > (\Gamma_i)_{316L} & \text{for } c_p \leq 30\% \\ (\Gamma_i)_{316L} > (\Gamma_i)_{788} & \text{for } c_p > 30\% \end{cases}$$

4. Discussion

None of these mechanical properties show any significant increase with respect to those of pure dense glass-ceramic. The question arises as to whether they are high enough for coating materials. This is difficult to answer about toughness and fracture energy; however, comments can be made on the strength.

In a first approximation, a stem of a prosthesis surrounded by a well-bound coating can be considered as a constant strain system. The most rigid component (the central metallic core) imposes its strain on the others. Accordingly, each layer is subjected to a stress proportional to its Young's modulus,

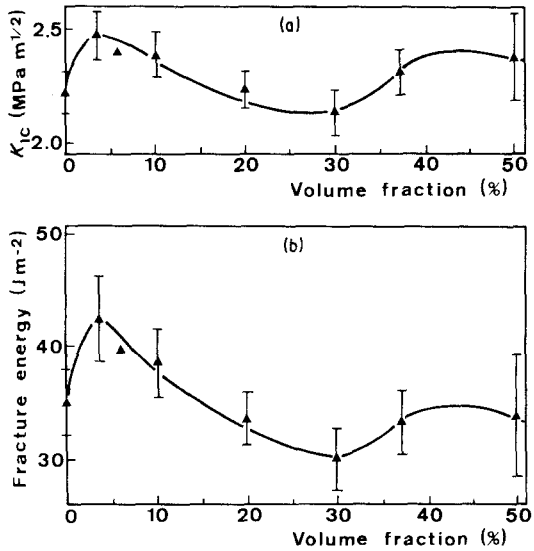

Figure 4 Fracture toughness (a) and fracture energy (b) of glass-ceramic (CAP)–titanium composites.

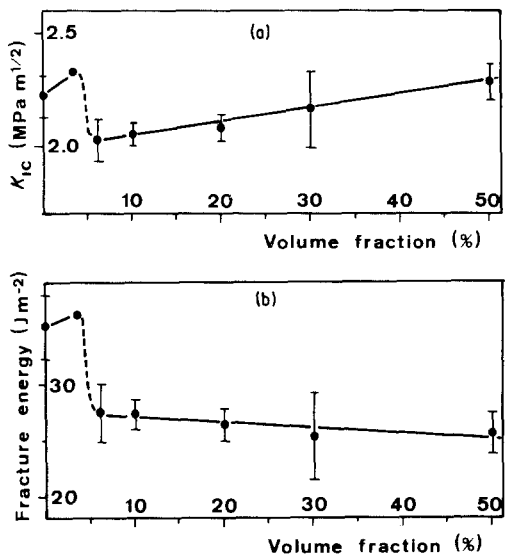

Figure 5 Fracture toughness (a) and fracture energy (b) of glass-ceramic (CAP)–316 L stainless steel composites.

since it has an elastic behaviour

$$\sigma_{layer} = \sigma_{metal} \frac{E_{layer}}{E_{metal}} \quad (13)$$

The maximum tensile stress, σ_{metal}, along the stem of hip prostheses depends both on design and material. These stresses are listed in Table IV for various stem types when they are implanted in fresh cadaver femur and loaded at 3000 N (about four times average body weight) on special equipment [15, 27]. Assuming these stems are surrounded by corresponding glass-ceramic–metal composite layers, each layer would withstand a tensile stress, σ_{layer}, given by Equation 13. These values are compared to the fracture stress $\sigma_{R,3}$ of composites: in all cases $\sigma_{R,3}$ is greater than σ_{layer}. However, $\sigma_{R,3}$ often overestimates the tensile strength of materials and therefore a comparison has been also made with $\sigma_{R,4}$, which better takes into account the distribution of microstructural flaws; in most cases,

TABLE IV Maximum tensile stress along the stem of various prostheses [27]

Type of prostheses	Material	Young's modulus (GPa)	Maximum tensile stress (Mpa)
Charnley curved standard	Forged 316 L	193	200
Müller curved standard	Cast CrCo (Hs21)	230	180
Charnley Kerboull No. 4	Forged 316 L	193	120
Müller straight 12.5	Forged MP35N (CoNiCr alloy)	230	115
Osteal DN	Forged TA 6 V (titanium alloy)	110	80

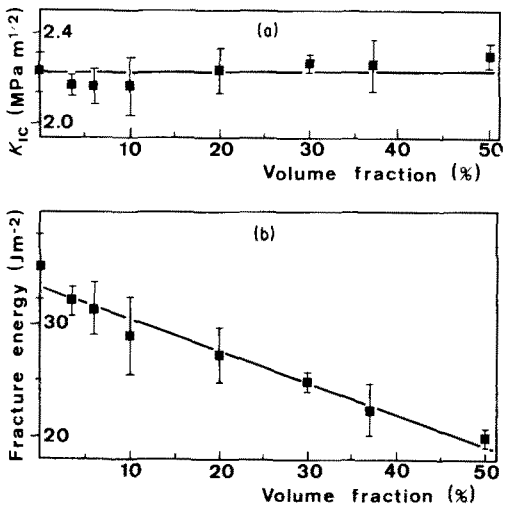

Figure 6 Fracture toughness (a) and fracture energy (b) of glass-ceramic (CAP)–cobalt–chromium 788 composites.

$\sigma_{R,4}$ is also greater than σ_{layer}. The best results are obtained with cobalt–chromium composites on the Müller straight stem: the ratio $R = \sigma_{R,4}/\sigma_{layer}$, which will be considered as a factor of security, is always greater than 2 and sometimes than 3. This ratio is about 2 for most other combinations. Only the most rigid 316 L and 788 composites on Charnley and Müller curved stems are definitely unsatisfactory ($R \leq 1.5$).

5. Conclusions

Bulk glass-ceramic CAP–metal particulate composites can be obtained from mixtures of calcium alumino-phosphate glass and various metals or alloys (titanium, 316 L stainless steel and cobalt–chromium 788 alloy) commonly used in orthopaedic or orthodontic surgery. They are prepared by hot pressing using a flash pressing technique. In each of the three systems, materials with various metal volume fractions (up to 50%) have been synthesized in this way. The elastic and thermal properties are within those of glass-ceramic CAP and those of corresponding metal.

Although their mechanical strength remains close to that of dense glass-ceramics, a simple calculation leads us to conclude that most composites could withstand about four times body weight when bound to suitable rigid metallic cores. However, this result should be confirmed by more accurate computations. To account for this approximation and for the fatigue phenomena, which have not yet been studied, and thus to increase the factor of safety, improvements could be made.

In glass-ceramic–titanium systems, as-received angular particles (Fig. 1a) should be replaced by small spherical ones. The probability of microcracking due to high thermal mismatch ($\Delta\alpha = +7.4 \times 10^{-6}\,°C^{-1}$), which depends both on the shape [28, 29] and the radius of particles [30–33], would be reduced and thus the mechanical properties would be increased significantly [33]. In other systems (CAP–316 L and CAP–788), the creation of an optimum matrix–particle bond, by suitably pre-oxidizing particles, would improve both strength and toughness [34, 35]. Preliminary experiments on a glass-ceramic–cobalt–chromium system give promising results. All these solutions would have the advantage of keeping particulates as reinforcement and thus making the use of special techniques easier, such as plasma spraying to bind composites to the stems.

The biocompatibility of composites, which has not yet been studied, should also appear as good as that of the components. With all these improvements and controls, such materials could be suitable to realize a thermal and elastic transition between a dense metallic stem and a porous glass-ceramic coating. A new type of direct anchoring prosthesis would thus be obtained which would compete favourably with porous metal coating devices.

Without regarding their prosthetic applications, such materials can also be studied as composite materials. The values of their elastic moduli and average linear thermal expansion coefficients can be compared with various theoretical curves, which give the evolution of these properties as a function of metal volume fraction, c_p, and the properties of individual phases. This will allow us to obtain information about the textures of various systems.

References

1. L. SMITH, *Arch. Surg.* **87** (1963) 653.
2. P. BOUTIN, *Rev. Chir. Orthop.* **58** (1972) 229.
3. S. F. HULBERT, F. A. YOUNG, R. S. MATHEWS, J. J. KLAWITTER, C. D. TALBERT and F. H. STELLING, *J. Biomed. Mater. Res.* **4** (1970) 433.
4. S. N. BHASKAR, J. M. BRADY, L. GETTER, M. F. GROMER and T. DRISKELL, *Oral Surg.* **32** (1971) 336.
5. P. W. McMILLAN, "Glass-Ceramics", 2nd edn (Academic, London, 1979).
6. L. L. HENCH, R. J. SPLINTER, W. C. ALLEN and T. K. GREENLEE, *J. Biomed. Mater. Res. Symp.* **2** (1971) 117.

7. F. PERNOT, J. ZARZYCKI, F. BONNEL, P. RABISCHONG and P. BALDET, *J. Mater. Sci.* **14** (1979) 1694.
8. F. PERNOT, P. BALDET, F. BONNEL, J. ZARZYCKI and P. RABISCHONG, *Ceram. Int.* **9** (1983) 127.
9. P. BALDET, F. PERNOT, J. ZARZYCKI, F. BONNEL and P. RABISCHONG, in "Biomaterials 80 – Advances in Biomaterials", Vol. 3, edited by G. D. Winter, D. F. Gibbons and H. Plenk, Jr (Wiley, New York, 1982) p. 73.
10. F. G. EVANS, "Mechanical Properties of Bone" (C. C. Thomas, Springfield, 1973).
11. A. K. VARSHNEYA, in "Treatise on Materials Science and Technology" Vol. 22, edited by M. Tomozawa and R. Doremus (Academic, New York, 1982) p. 241.
12. A. ROTH, "Vacuum Sealing Techniques" (Pergamon, London, 1966).
13. S. TIMOSHENKO and J. N. GOODIER, in "Theory of Elasticity", 2nd edn (McGraw-Hill, New York, 1951) p. 23.
14. P. DUCHEYNE and L. L. HENCH, *J. Mater. Sci.* **17** (1982) 595.
15. P. CHRISTEL, A. MEUNIER, S. LECLERCQ, P. BOUQUET and B. BUTTAZZONI, *J. Biomed. Mater. Res., Appl. Biomat.* **21** (1987) 191.
16. M. DECOTTIGNIES, J. PHALIPPOU and J. ZARZYCKI, *J. Mater. Sci.* **13** (1978) 2605.
17. J. F. W. BELL, A. C. JOHNSON and J. C. K. SHARP, *J. Acoust. Soc. Amer.* **57** (1975) 1085.
18. J. F. W. BELL and J. M. PELMORE, *J. Phys. E: Sci. Just.* **10** (1977) 1145.
19. H. J. McSKIMIN, in "Physical Acoustics", Vol. 1, Part A, edited by W. P. Mason (Academic, New York, 1964) p. 271.
20. W. F. BROWN and J. E. SRAWLEY, in ASTM Special Technical Publication no. 410, (ASTM, Baltimore, 1967) p. 1.
21. J. L. CHERMANT, F. OSTERSTOCK and G. VADAM, *Verres Réfract.* **33** (1979) 843.
22. N. MIYATA and H. JINNO, *J. Mater. Sci.* **16** (1981) 2201.
23. J. R. VAN WAZER, "Phosphorous and its Compounds" (Interscience, New York, 1958).
24. A. J. LEADBETTER and T. W. SMITH, *Phil. Mag.* **33** (1976) 105.
25. V. G. KOMLEV, I. D. KURKINA and V. A. PETROV, Ogneupory **12** (1979) 46.
26. W. F. HORN and F. A. HUMMEL, *J. Amer. Ceram. Soc.* **63** (1980) 338.
27. P. S. CHRISTEL, A. MEUNIER, D. BLANQUAERT, J. WITVOET and L. SEDEL, *J. Biomed. Engng.* **10** (1988) 57.
28. R. R. TUMMALA and A. L. FRIEDBERG, *J. Amer. Ceram. Soc.* **52** (1969) 228.
29. I. W. DONALD and P. W. McMILLAN, *J. Mater. Sci.* **11** (1976) 949.
30. R. W. DAVIDGE and T. J. GREEN, *ibid.* **3** (1968) 629.
31. F. F. LANGE, in "Fracture Mechanics of Ceramics", Vol. 2, edited by R. C. Bradt, D. P. H. Hasselman and F. F. Lange (Plenum, New York, 1974) p. 599.
32. V. D. KRSTIC and M. D. VLAJIC, *Acta Metall.* **31** (1983) 139.
33. N. MIYATA, K. TANIGAWA and H. JINNO, in "Fracture Mechanics of Ceramics" Vol. 5, edited by R. C. Bradt, D. P. H. Hasselman and F. F. Lange (Plenum, New York, 1983) p. 609.
34. M. A. STETT and R. M. FULRATH, *J. Amer. Ceram. Soc.* **53** (1970) 5.
35. A. K. KHAUND and P. NICHOLSON, *J. Mater. Sci.* **15** (1980) 177.

Received 20 July
and accepted 22 November 1990